NUCLEAR SCIENCE AND TECHNIQUES **25**, 030403 (2014)

A nuclear spectrum generator for semiconductor X-ray detectors*

ZENG Guo-Qiang (曾国强),[1,†] TAN Cheng-Jun (谭承君),[1] LUO Qun (罗群),[1]
GE Liang-Quan (葛良全),[1] LI Chen (李晨),[1] GONG Chun-Hui (龚春慧),[1] and LIU Xi-Yao (刘玺尧)[1]

[1] *Chengdu University of Technology, Chengdu 610051, China*

(Received October 3, 2013; accepted in revised form December 18, 2013; published online June 20, 2014)

A nuclear spectrum generator for semiconductor X-ray detectors is designed in this paper. It outputs step ramp signals with random distribution in amplitude and time according to specified reference spectrum. The signals are similar to the signals from an actual semiconductor X-ray detector, and can be use to check spectrum response characteristics of an X-ray fluorometer. This helps improving energy resolution of the X-ray fluorometer. The spectrum generator outputs step ramp signals satisfying the probability density distribution function of any given reference spectrum in amplitude through sampling on the basis of 32-bit randomizer. The system splits 1024 interval segmentation of the time that the step ramp signals appear, and calculates the appearance probability of step ramp signals in different intervals and the average time between the time intervals, by random sampling. The step ramp signals can meet the rule of exponential distribution in time. Test results of the spectrum generator show that the system noise is less than 2.43 mV, the output step ramp signals meet the Poisson distribution in counting rate and the probability density distribution function of the reference spectrum in amplitude. The counting rate of the output step ramp signals can be adjusted. It meets the rule of the output signals from semiconductor X-ray detectors, such as Si-pin detector and silicon drift detector.

Keywords: X-ray spectrum generator, Random sampling, Probability density distribution, Poisson distribution

DOI: 10.13538/j.1001-8042/nst.25.030403

I. INTRODUCTION

As an important equipment for nondestructive analysis of materials, portable X-ray fluorometer is widely used in mining, dressing, smelting, petrochemical, environmental protection, commodity inspection, archaeology, medicine, etc. [1, 2], and how to improve its performance is an unceasing pursuit of hardware researchers.

An X-ray fluorometer is composed of an X-ray source, a detector and a multi-channel analyzer (MCA). Many factors affect energy resolution of an X-ray spectrum, such as statistical fluctuations of the interaction between X-ray and the detector, the detector's inherent energy resolution, and electronics noise of preamplifier and MCA, etc. [2] High resolution nuclear instruments are made of good detectors and electronics components, but reduced electronics noise and improved energy resolution can be achieved with the inverse convolution method, too, such as simulating the output signals of semiconductor alpha detector by Fernández Timón *et al.* in 2010 [3].

MCA produces electronics noise and ballistic deficit in its signal processing, hence the loss in energy resolution of fluorometer [4–6]. To improve the resolution with the inverse convolution method is actually to treat the MCA board as a linear system and obtain the theoretical spectrum ($f1[n]$) through inverse convolution of the measured spectrum ($y1[n]$) and the system response function ($h[n]$), with the known response function ($h[n]$) of the MCA system [7]. The theoretical spectrum is of the highest energy resolution the X-ray detector's output can reach, ignoring effect of the MCA electronics noise and the ballistic deficit. The schematic block diagram of the inverse convolution method is shown in Fig. 1.

For improving the system energy resolution with the inverse convolution method, the first prerequisite is to obtain the system response function ($h[n]$) of the MCA board. Therefore, a step ramp signal generator of standard spectrum (known as the standard spectrum generator) is required. The measured spectral line of the target MCA on the standard spectrum can be obtained by transferring step ramp signals from the standard spectrum generator to the target MCA. Next, the system response function of the target MCA is obtained by the inverse convolution calculation of the measured spectral line and the standard one. Then, the system response function is applied in the actual engineering survey to improve the system energy resolution. All these are based on assuming the MCA as a linear system. However, this is true only if the count rate of step ramp signals is within a certain range [8]. Thus, it is necessary to measure the system response function of MCA in different count rate ranges to meet requirements of practical applications. In this paper, a standard spectrum generator is designed according to the above requirements for applications to semiconductor X-ray detectors.

Spectrum generator is the basis for improving energy resolution of fluorometers by the inverse convolution method. Its output step ramp signal should be the same as that of semiconductor X-ray detector. It should meet: 1) the distribution in amplitude of the step ramp signals from the spectrum generator should be spectrum of random reference (i.e. the probability density distribution function) given by host computer; 2) the step ramp signal should satisfy the exponential distribution in time [9]; 3) the output step ramp signal count rate

* Supported by National High Technology Research and Development Program of China (No. 2012AA061803) and Middle-aged and Young Backbone Teacher of Chengdu University and Technology (No. JXGG201408) and Science and technology project of CDUT (No. 2013KL035)

† Corresponding author, zgq@cdut.edu.cn

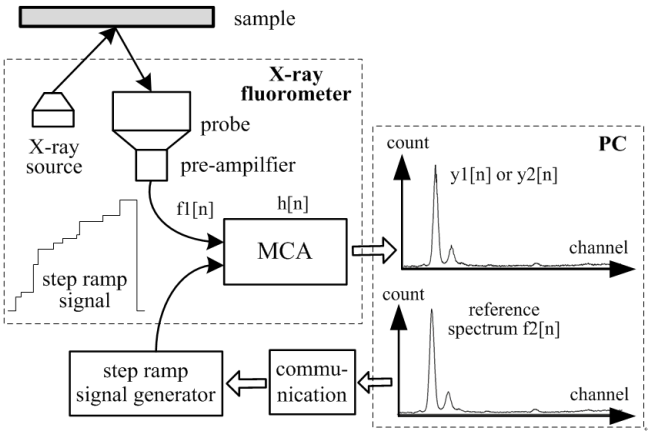

Fig. 1. Sketch of an XRF system.

is adjustable; 4) the rising edge of output signal is less than 100 ns; 5) the voltage swing of output signal is about ±2 V and the amplitude resolution is better than 1 mV; and 6) the system noise is below 4 mV.

Tremendous amounts of work were done on simulating the nuclear pulse signal output from γ-ray detectors. For example, Attwenger *et al*. [10] built a nuclear pulse signal generator directly through using a analog circuit in 1969, and Yang *et al*. [11] developed a nuclear pulse signal generator in 1996 by using single chip microcomputer. However, the traditional nuclear signal generators simulating output signal of γ-rays, which is usually bi-exponential, cannot satisfy the probability density distribution function of any given reference spectrum in amplitude. Therefore, the traditional signal generators cannot meet the test requirements or solve the system response function of the X-ray fluorometer.

To the authors' knowledge, researches on simulating output step ramp signal of semiconductor X-ray detector have not been reported. In this paper, a spectrum generator is designed with the random sampling method on the basis of the randomizer. The spectrum generator can be used for testing both the system response function of an MCA board and its maximum pulse passing rate, linearity [12], ability of pulse pile-up rejection, etc. [13], so as to realize the correction of various performance indexes of fluorometer [14, 15]. In addition, the spectrum generator can generate various discrete nuclear signal waveforms, and researches of parameter detection, frequency spectrum analysis and other digital processing algorithms of nuclear signals can be conducted [16, 17].

II. HARDWARE DESIGN SCHEME OF THE SYSTEM

The hardware design scheme of this system is realized based on the FPGA. The circuit is shown in Fig. 2 (FPGA was not involved in it in order to represent the analog circuit design clearly). The system takes FPGA as the core and high-speed DAC as the signal output module. The step ramp signal can be obtained after the amplifier circuit processing of the output signal from the DAC.

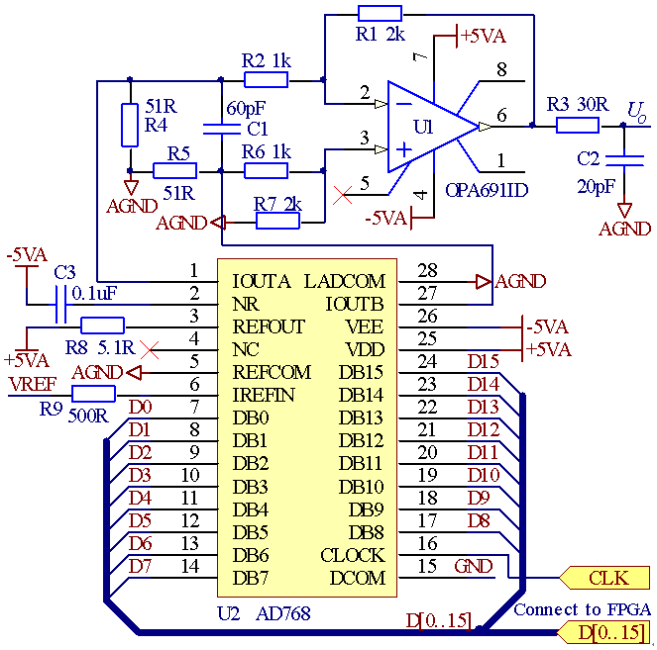

Fig. 2. (Color online) Hardware circuit of the system.

The FPGA realizes the communication with host computer to get the reference spectral data (i.e. the probability density distribution function of the output step ramp signal in amplitude) and the average count rate of the output step ramp signal. Then, to make a random sampling, the sampling data in amplitude and time are calculated. Finally, the FPGA outputs the control signal to high speed DAC, which outputs the corresponding current signals. After amplification, the generator outputs the step ramp signal which obeys the probability density distribution in amplitude and the exponential distribution in time.

Since the rising edge of output signal of semiconductor X-ray detector is less than 100 ns, the settling time of the selected DAC and operational amplifier (OPAMP) shall be within 100 ns, and the bandwidth of OPAMP shall be over 100 MHz (including 10 times margin). Since the voltage swing of output signal of semiconductor X-ray detector is ±2 V, the slew rate (SR) of OPAMP shall be greater than 40 V/μs. Furthermore, the chip shall be of the best linearity available since the system linearity affects the goodness-of-fit between output signal spectrum and reference spectrum. After comprehensive consideration, we selected the current-output AD768 as the DAC, which is of high resolution (16-bit), fast speed (30 MSPS), short settling time (25 ns full-scale settling to 0.025%) and good linearity (1/2 LSB DNL@14 bits, 1 LSB INL@14 bits) [18]. Additionally, a current-feedback OPAMP (OPA691) was selected as signal conditioning chip which is of large bandwidth (190 MHz@G=2), high SR (2100 V/μs), low noise (when $f > 1$ MHz, $u_{\rm NI} = 2.9\,{\rm nV}/\sqrt{\rm Hz}$, $i_{\rm NI} = 15{\rm pA}/\sqrt{\rm Hz}$) and short settling time (12 ns, $V_{\rm O} = 2$ V step settling to 0.02%) [19].

According to the data sheet of AD768 [18] and design scheme in Fig. 2, when the digital signal input in AD768 is

CODE, the voltage of corresponding output signal is

$$U_{\rm o} = \frac{R_1}{R_2}(I_{\rm OUT,B}R_5 - I_{\rm OUT,A}R_4), \tag{1}$$

where $I_{\rm OUT,B}$ and $I_{\rm OUT,A}$ are the output current signals of AD768 at pin 1 and 27, respectively, when the digital signal input in AD768 was *CODE*. According to Fig. 2, $R_4 = R_5$. Therefore, Eq. (1) can be changed into

$$U_{\rm o} = \frac{R_1}{R_2}R_4\frac{2CODE - 2^{16}}{2^{16}} \times 4 \times \frac{V_{\rm REF}}{R_9}, \tag{2}$$

where $V_{\rm REF}$ is the external reference voltage source (2.5 V) and $V_{\rm REF}/R_9$ is the reference current source of AD768. From Eq. (2), amplitude resolution of the system is $0.0763\,{\rm mV}$, satisfying requirement of the system; according to the data sheet of AD768, the integral and differential nonlinearities brought by AD768 at the 14-bit resolution are $0.305\,{\rm mV}$ and $0.153\,{\rm mV}$, respectively, satisfying requirement of the system, too.

III. CONTROL OF THE STEP RAMP SIGNAL IN AMPLITUDE AND TIME

A spectrum generator should solve two problems: what the amplitude of the next one is and when the next one shall be output, after one step ramp signal is output.

To solve the two problems, it needs to start with the distribution characteristics of the step ramp signal in amplitude and time. The step ramp signal is actually the signal detected by semiconductor detector when an excited atom sends out the characteristic X-ray during de-excitation. According to the law of atomic transition, the signal meets the exponential distribution in time [9], and thesignal amplitude meets the probability density distribution function of the reference spectrum given by the host computer.

The control scheme of the step ramp signal in amplitude and time will be introduced as follows.

A. Control algorithm of the step ramp signal in amplitude

In amplitude, the output step ramp signal satisfies the probability density distribution function of the reference spectrum. The host computer gives different reference spectrums and amplitudeof the output step ramp signal isof different probability density distribution functions, hence the random sampling control scheme of amplitude.

It is assumed that conversion gain of the signal is $10\,{\rm mV/keV}$, the maximum X-ray energy in the measurement of the spectral line is $50\,{\rm keV}$, and the resolution of the spectral line is 1024. In terms of the reference spectrum line $data[1024]$ given by host computer, the occurrence probability of the step ramp signal corresponding to the $n^{\rm th}$ channel ($n = 0, 1, 2, \ldots, 1023$) is the counts of the $n^{\rm th}$ channel $data[n]$ divided by the total counting number $data\_sum[1023]$ of $data[1024]$,

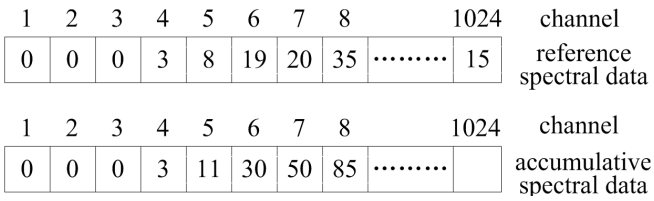

Fig. 3. The scheme of sampling probability density distribution.

namely, $data[n]/data\_sum[1023]$; the amplitude of the step ramp signal corresponding to the $n^{\rm th}$ channel is $500(n + 1)/1024\,{\rm mV}$.

The system sampling in amplitude and time is implemented based on randomizer. The random numbers generated by randomizer is evenly distributed, in other words, the numbers generated enjoy the equal probability. In order to obtain different probabilities, the system needs to distribute different data intervals. As shown in Fig. 3, there are two arrays: the reference spectrum line $data[1024]$(the probability density distribution function in amplitude) is obtained from host computer, and the cumulative spectral line $data\_sum[1024]$. The value of the cumulative spectral data of the $n^{\rm th}$ channel $data\_sum[n]$ is the accumulation of the reference spectral data in thefirst$n$channels. So, the difference of accumulative spectrum data between the $n^{\rm th}$ channel and the $(n-1)^{\rm th}$ channel ($data\_sum[n] - data\_sum[n-1]$) is equal to the $n^{\rm th}$ channel value of the reference spectrum line $data[n]$. Therefore, the probability of a random number with a range of $0 \sim data\_sum[1023]$ appearing between the values of the accumulative spectrum data in the $(n-1)^{\rm th}$ and $n^{\rm th}$ channels $(data\_sum[n] - data\_sum[n-1])/data\_sum[1023]$ is equal to the probability that the step ramp signal of the $n^{\rm th}$ channel of the reference spectrum data appearing when being output $(data[n]/data\_sum[1023])$. Thus, the system determines the amplitude of the output step ramp signal through searching the range of the random number in the accumulative spectrum data. The specific process of the amplitude sampling is as follows:

A 32-bit pseudo-random number p is generated by randomizer in the FPGA. Then, the random number p takes the remaining of $data\_sum[1023]$ to get a random number qwith the range of $0 \sim data\_sum[1023]$. Finally, the successive approximation approach is used to search the range of the random number q in the cumulative spectrum data. If the random number q is between $data\_sum[n-1]$ and $data\_sum[n]$, the amplitude of the output signal should be $500n/1024{\rm mV}$, thus realizing the probability density function distribution in amplitude.

The premise of the above analysis is that the random number q is evenly distributed in the range of $0 \sim data\_sum[1023]$. However, if maximum random number M generated by the randomizercannot be divisible by $data\_sum[1023]$, the smaller random number q is more possible to appear in the range of $0 \sim data\_sum[1023]$ than the greater one, rather than the absolute even distribution. It is set

TABLE 1. Time sampling parameters of the output step ramp signal ($m = 52.194$k/s)

Start time c (μs)	Terminal time d (μs)	Probability $P_{(d>t>c)}$	Multiply 10 000 000 $data\_pro[1024]$	Average time $\bar{t}_{(d>t>c)}$/ns $data\_time[1024]$
0.1	0.2	0.0051787022	51787	100.7766
0.2	0.3	0.0051517429	51517	201.2877
0.3	0.4	0.0051249240	51249	301.7935
0.4	0.5	0.0050982446	50982	402.2940
0.5	0.6	0.0050717042	50717	502.7892
0.6	0.7	0.0050453019	50453	603.2792
0.7	0.8	0.0050190370	50190	703.7641
0.8	0.9	0.0049929089	49929	804.2438
0.9	1.0	0.0049669168	49669	904.7184
1.0	1.1	0.0049410600	49411	1005.1879
1.1	1.2	0.0049153378	49153	1105.6524
1.2	1.3	0.0048897496	48897	1206.1120
1.3	1.4	0.0048642945	48643	1306.5666
1.4	1.5	0.0048389719	48390	1407.0163
1.5	1.6	0.0048137812	48138	1507.4612
1.6	1.7	0.0047887216	47887	1607.9012
1.7	1.8	0.0047637925	47638	1708.3364
1.8	1.9	0.0047389931	47390	1808.7669
1.9	2.0	0.0047143228	47143	1909.1927

by Eq. (3)

$$M \div data\_sum[1023] = R \cdots S, \tag{3}$$

where, R is the quotient, S is the remainder and $S \neq 0$. Then, the probability of the random data q appears in $1 \sim S$ is $1/R$ larger than that in $S+1 \sim data\_sum[1023]$, indicating the uneven probability.

The maximum random number $M = 2^{32} - 1$ is generated by the 32-bit randomizer. In the case that the total counts of the reference spectrum line $data\_sum[1023]$ is not over 1 000 000, the error probability (1/R) will be less than:

$$1000000/(M - M\%1000000) \approx 0.00023288, \tag{4}$$

where % is the remainder. The error probability of <0.023% is acceptable. Also, Eq. (4) shows that the more bit the randomizerhas, the smaller the error probability $(1/R)$ will be. In addition, adjustment can be made according to the random number p generated by the randomizer in the FPGA to eliminate the error probability $(1/R)$. If the random number p is within the range of $0 \sim (M - M\%data\_sum[1023])$, the following data sampling work can be continued; or this random number should be abandoned and a new one should be generated.

B. Control algorithm of the step ramp signal in time

The step ramp signal obeys Poisson distribution in count rate. In other words, when the average count rate is$m$, the probability that the output signals appear n step signals within the time of $t$can be written as [9]:

$$P(t,n) = \frac{(mt)^n}{n!}\mathrm{e}^{-mt}. \tag{5}$$

The condition that two adjacent step ramp signals appear at the time interval of t is: no step ramp signal appears within the time of t after the first one (the probability is $P(t,0)$); one step ramp signal appears in the following $\mathrm{d}t$ time (the probability is $P(\mathrm{d}t,1)$). Since the two events above are independent of each other, the probability $\mathrm{d}P(t)$ of two adjacent step ramp signals appearing at the time interval of t is:

$$\begin{aligned} \mathrm{d}P(t) &= P(t,0)P(\mathrm{d}t,1) \\ &= \frac{(mt)^0}{0!}\mathrm{e}^{-mt} \times \frac{(m\mathrm{d}t)^1}{1!}\mathrm{e}^{-m\mathrm{d}t} \\ &\approx m\mathrm{e}^{-mt}\mathrm{d}t. \end{aligned} \tag{6}$$

Therefore, the probability of appearing the step ramp signals at the time interval of (c,d) is:

$$\begin{aligned} P_{(d>t>c)} &= \int_c^d \mathrm{d}P(t) \\ &= \mathrm{e}^{-mc} - \mathrm{e}^{-md}. \end{aligned} \tag{7}$$

The average time of the time interval (c,d) is:

$$\begin{aligned} \bar{t}_{(d>t>c)} &= c + \int_c^d t\mathrm{d}P(t) \\ &= c + (c + \frac{1}{m})\mathrm{e}^{-mc} - (d + \frac{1}{m})\mathrm{e}^{-md}. \end{aligned} \tag{8}$$

After the firststep ramp signal is output, the system will divide the time period so that the second one may appear into x intervals,and the average time of each time interval and the probability that it appears in different time intervals are calculated by Eqs. (8) and (7), see Table 1. Then, it makes the random sampling according to the probability that the step ramp signal appears in different time intervals. If the time obtained by sampling is 1.5–1.6 μs, when will the next step ramp

signal be output? It is necessary to take the average time of 1.5–1.6 μs as its appearance time. Table 1 lists the probability that the step ramp signal appears in different time intervals and the average time of the time interval when the average count rate $m = 52.194$ k/s and the time interval $x = 1024$. It should have 1024 data, but owing to the limitation of space, only the data of 19 time intervals are listed.

The data in the last two columns of Table 1 are used for time sampling in the FPGA. The time sampling process within the FPGA is as follows: the time sampling mode is divided the time of the step ramp signal appears into 1024 intervals according to the average count rate m; the probability (Column 3 of Table 1) that the step ramp signal appears in different time intervals and the average time $data\_time[1024]$ (Column 5 of Table 1)in the time interval are obtained by Eqs. (7) and (8); next, the probabilityis multiplied by a base number $K = 10\,000\,000$ and the results are stored in the array $data\_pro[1024]$ (namely, the time probability distribution array, Column 4 of Table 1); then, a cumulative time probability distribution array $data\_pro\_sum[1024]$ is established, In the array, the data $data\_pro\_sum[n]$ is equal to the accumulative value of the first$n$ data of the array $data\_pro[1024]$. So the value of base number K is equal to the total counts $data\_pro\_sum[1023]$ of the array $data\_pro[1024]$ in theory.

Next, a random number p is generated by the randomizer, and the random number q within the range of $0 \sim data\_pro\_sum[1023]$ is obtained by letting the random number p take the remaining of the total counts $data\_pro\_sum[1023]$ of the array $data\_pro[1024]$; finally, the successive approximation approach is used to search the range of the random number q in the cumulative time probability distribution array $data\_pro\_sum[1024]$. If the random number q is between the $data\_pro\_sum[n]$ and $data\_pro\_sum[n+1]$, the output time of the next step ramp signal should be $data\_time[n+1]$, thus realizing the output of the step ramp signals according to the exponential distribution in time.

Like the amplitude sampling, the sampling for time also needs to consider the case of the uneven probability distribution when the maximum random number M cannot be divisible by the total counts $data\_pro\_sum[1023]$ of the array $data\_pro[1024]$. In fact, the base number K can be selected which can make the maximum random number M be divisible by $data\_pro\_sum[1023]$, such as 1 114 129; 3 342 387; 5 570 645, rather than 10 000 000.

In addition, according to the test results, the greater the time division interval x is, the closer the distribution of the output step ramp signals in count rate is to the Poisson distribution; but too large time interval x will lead to the increase of the storage space in the FPGA and the time of searching the range of the random number q, thus occupying more resources of the FPGA and reducing the count rate of the output signals. Taking all into account, it is appropriate to take the time division interval of $x = 1024$.

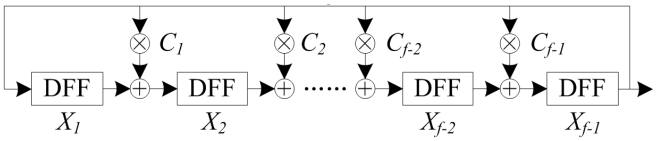

Fig. 4. Schematic diagram of the LFSR.

TABLE 2. Feedback matrixes when $e = 32$, $f = 45 \sim 50$ [20]

f	Subscript when $C_i =$ "1"	Number of "1" in in $\boldsymbol{T}^e$	Length of longest feedback chain in $\boldsymbol{T}^e$
45	44, 43, 41, 40	357	18
46	45, 44, 25, 24	534	27
47	46, 41	166	8
48	47, 46, 20, 19	589	27
49	48, 39	123	5
50	49, 48, 13, 22	589	29

C. Design of randomizer in FPGA [20]

This system uses linear feedback shift register (LFSR) to produce uniformly distributed random numbers. The design of LFSR is shown in Fig. 4, where the feedback factor $C_i (1 \le i \le f-1)$ adopts the binary system ("0" or "1"). Add operation ignores the carry and multiply operation is a selecting operation.

The equation of shifting register in Fig. 4 can be expressed as:

$$\begin{bmatrix} X_0(t+D) \\ X_1(t+D) \\ X_2(t+D) \\ \vdots \\ X_{f-3}(t+D) \\ X_{f-2}(t+D) \\ X_{f-1}(t+D) \end{bmatrix} = \begin{bmatrix} 0 & 0 & \dots & 0 & 0 & 1 \\ 1 & 0 & \dots & 0 & 0 & C_1 \\ 0 & 1 & \dots & 0 & 0 & C_2 \\ \vdots & \vdots & \ddots & \vdots & \vdots & \vdots \\ 0 & 0 & \dots & 1 & 0 & C_{f-3} \\ 0 & 0 & \dots & 0 & 1 & C_{f-2} \\ 0 & 0 & \dots & 0 & 0 & C_{f-1} \end{bmatrix} \begin{bmatrix} X_0(t) \\ X_1(t) \\ X_2(t) \\ \vdots \\ X_{f-3}(t) \\ X_{f-2}(t) \\ X_{f-1}(t) \end{bmatrix}, \tag{9}$$

where D is one clock delay:

$$\boldsymbol{X}(t+D) = \boldsymbol{T}\boldsymbol{X}(t). \tag{10}$$

Generally, a randomizer with e bits needs e clock cycles to produce a random number. To speed up the random number production, we iterate Eq. (10) for e $(e < f)$ times:

$$\boldsymbol{X}(t+eD) = \boldsymbol{T}^{\boldsymbol{e}}\boldsymbol{X}(t). \tag{11}$$

Therefore, random number with e bits can be gained in a clock cycle when taking $\boldsymbol{T}^e$ as the feedback network. In this system, $e = 32$, while f is determined by the complexity of the feedback network. The complexity of the feedback network with$f$ ranging between $45 \sim 50$ is listed in Table 2. When $f = 49$, $\boldsymbol{T}^e$ has the least "1" and its longest feedback chain is the shortest. As a result, this system selects to use 49 shifting registers.

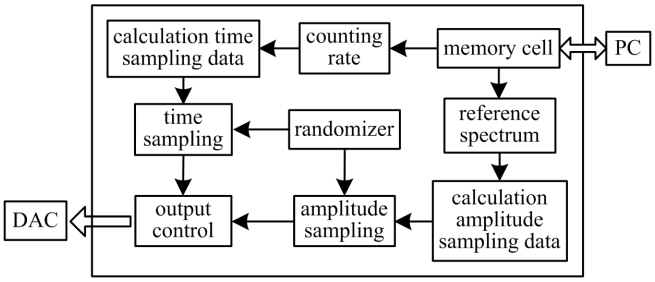

Fig. 5. Logic control block diagram in the FPGA.

TABLE 3. Logic consumption in the FPGA.

Logic resource	Logic consumption
Total logic elements	2749/8256(33%)
Total registers	221
Total memory bits	73728/165888(44%)
Total PLLs	1/2(50%)

D. Logical design of amplitude and time sampling in FPGA

According to the theoretical calculation and method introduction of time and amplitude sampling above, a hardware logical control block diagramwithin the FPGA is designed, as shown in Fig. 5.

The diagram is mainly composed of storage, randomizer, amplitude sampling block, time sampling block and output control. The PC sends the reference spectral data and the average count rate to the FPGA for storage via the serial port. The time sampling block divides the time into 1024 intervals and obtains the probability that step ramp signal appears in each time interval and the average time during the interval according to the average count rate.Then, it samples times to obtain the time of the next step ramp signal appears. The amplitude sampling block obtains the cumulative spectrum data according to the reference one and samples amplitudes to get the amplitude of the next step ramp signal. The output control block obtains the sampling time and sampling amplitude and output the step ramp signal. EP2C8T144C8N is used as the FPGA chip in the system. When the system clock is working at 100 MHz, the FPGA logical resources of EP2C8T144C8N are shown in Table 3.

The randomizer, time sampling block, amplitude sampling block and output control can be implemented in parallel with a pipeline structure in the FPGA, which greatly improves the output speed of the output signal.

IV. TEST RESULTS

According to the characteristics of step ramp signals, the system test mainly includes the waveform, noise,amplitude distribution and time distribution of the output step ramp signals.

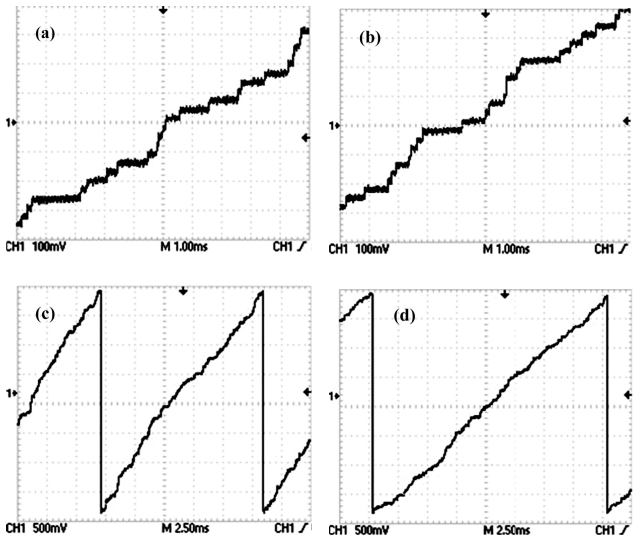

Fig. 6. Comparison of the signals output from the silicon drift detector and spectrum generator.

A. Test of the waveform of the output signal

Figures 6(a) and 6(c) are output signals from silicon drift detector (SDD), while Figs. 6(b) and 6(d) are output signals from spectrum generator. The counting rate of the signals is about 2.5 k/s. From Fig. 6, one sees that the output signals from the SDD and spectrum generator are almost the same, thus satisfying the actual use.

B. System noise test

Noise of nuclear spectrum generator can be tested by noise widening of signal amplitude spectrum. Control the nuclear spectrum generator to output a series of constant-amplitude step signals and input them into MCA to gain the amplitude spectrum. The full width at half maximum ($FWHM_x$) of this amplitude spectrum represents the signal noise. The MCA shall be scaled before the noise test: control the nuclear spectrum generator to output two kinds of constant-amplitude signals (V_{P1} and V_{P2}) and gain their corresponding peak positions (x_1 and x_2) through the MCA. Then, the voltage of each channel is $(V_{P1}-V_{P2})/(x_1-x_2)$. Therefore, noise expressed by voltage is:

$$FWHM_{NV} = (V_{P1}-V_{P2})FWHM_x/(x_1-x_2). \quad (12)$$

The physical testing system is shown in Fig. 7. Module (a) is the designed nuclear spectrum generator and module (b) is the digital multichannel analyzer (DMCA). In the DMCA, the shaping time constant of CR differential is 3.2 μs and the shaping time of RC integral is 25 μs. According to the above-mentioned test method, when the signal output rate of the system was about 10 k/s, the system noise calculated by Eq. (12) is 2.43 mV, indicating higher performance of the system.

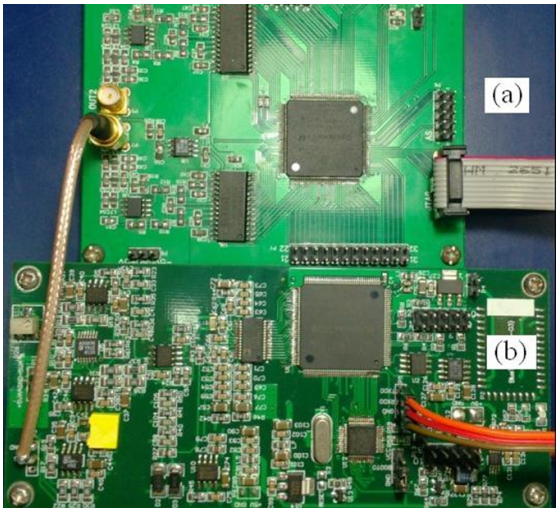

Fig. 7. (Color online) The testing system.

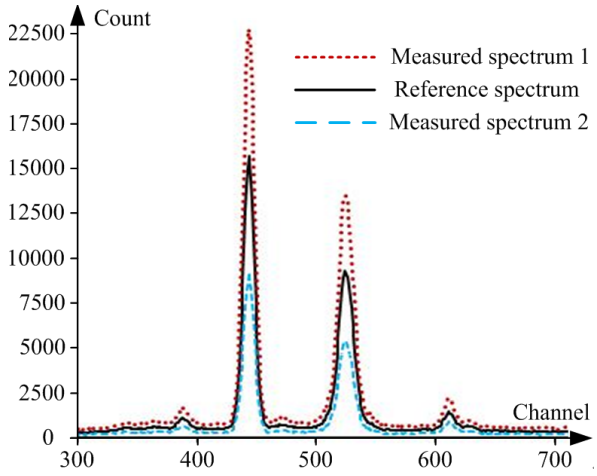

Fig. 8. (Color online) Comparison of test and reference spectra.

C. Amplitude distribution of the output signal

According to the above analysis, the output step ramp signal should satisfy the probability density distribution function of the given reference spectrum data in amplitude. X-ray fluorescence spectrum of a gold jewellery was taken as the reference spectrum. The gain of the output signal was adjusted; and the step ramp signals were output at the speed of 2 k/s. The output step ramp signals of the system were tested by a digital X-ray fluorometer and the spectra obtained indifferenttestingtimes were compared with the reference one. As shown in Fig. 8, the black solid line is the reference spectrum, and the two dotted lines refer to spectrum No. 1 and No. 2, obtained atthe total counts of 1 000 000 and 400 000, respectively. According to the figure, the waveform of the measured spectra is basically consistent with that of the reference one. The resolution of three lines should be 1024 channel, but only the counts of 300 to 700 channels are given in Fig. 8, for showing the three spectra more clearly.

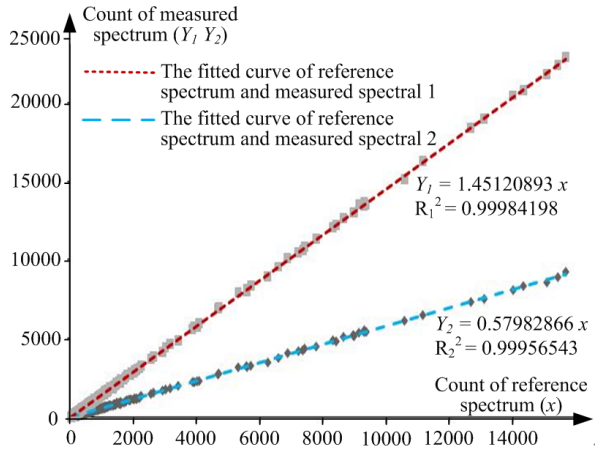

Fig. 9. (Color online) Linear fitting of test and reference spectra.

TABLE 4. The linear fitting coefficients error analysis of test spectrum and reference spectrum

Spectrum	Total count	Theoretical fitting coefficient	Actual fitting coefficient	Relative errors (%)
No.1	1 000 000	1.45067137	1.45120893	0.03705590
No.2	400 000	0.58026855	0.57982866	−0.07580771

TABLE 5. The outputs pulse signal error analysis of actual distribution and theoretical distribution in counting rate

Step signal number at the measurement time of 1 ms/n	Theoretical probability	Times of n step signals appearance at the measurement times of 100 000	Probability of n step signals appearance at the measurement times of 100 000	Relative errors (%)
43	0.025643194	2596	0.02596	−1.23544
44	0.030418656	3085	0.03085	−1.41802
45	0.035281585	3524	0.03524	0.11787
46	0.040032328	4027	0.04027	−0.59370
47	0.044456326	4446	0.04446	−0.00826
48	0.048340697	4781	0.04781	1.09783
49	0.051491721	5148	0.05148	0.02276
50	0.053751178	5407	0.05407	−0.59314
51	0.055009588	5584	0.05584	−1.50958
52	0.055214816	5509	0.05509	0.22606
53	0.054375134	5369	0.05369	1.26001
54	0.052556588	5302	0.05302	−0.88174
55	0.049875246	5058	0.05058	−1.41303
56	0.046485511	4663	0.04663	−0.31083
57	0.042566048	4239	0.04239	0.41359
58	0.03830504	3797	0.03797	0.87466
59	0.033886327	3371	0.03371	0.52035
60	0.029477715	2962	0.02962	−0.48268
61	0.025222293	2485	0.02485	1.47605
62	0.021233103	2129	0.02129	−0.26796
63	0.01759112	1788	0.01788	−1.64219
64	0.014346108	1419	0.01419	1.08816
65	0.011519704	1154	0.01154	−0.17618

In addition, a linear fitting was done between the reference spectrum and each of the measured spectra. As shown in Fig. 9, each fittingh as a linearity of 0.9995. The reference spectrum has a total counts of 689 336. The total counts of the spectrum No. 1 and No. 2, and their fitting coefficient and relative errors, are givenin Table 4. The relative error of the fitting coefficient of the measured spectra is within $\pm 0.076\%$. Therefore, the step ramp signals output by this step ramp signal generator satisfy the probability density distribution function of the reference spectrum data in amplitude.

D. Time distribution of the output signal

Eq. (5) is the Poisson distribution. The law of counting rate distribution of the step ramp signals were compared with the Poisson distribution. The results aregiven in Table 5. The data were obtained at 52.194 k/s of the counting rate of the output step ramp signal, measuring for 100 000 times and each time for 1 ms. Under this condition, the probability is the largest when the count is 52. It can be seen from Table 5 that in the case of a large number of repeated tests (measuring for 100 000 times), the measured probability of different counts is basically consistent with theoretical probability of the Poisson distribution. The maximum relative error is $\pm 1.65\%$, achieving the satisfactory result. The relative error will be smaller byincreasing the time of measurement. Therefore, the output of this step ramp signal generator satisfies the Poisson distribution in counting rate. Limited to space, only the probability of 43 to 65 step signals at the measurement time of 1 ms and the relative error are shown in Table 5.

V. CONCLUSION AND DISCUSSION

An arbitrary X-ray fluorescence spectrum generator has been developed. The step ramp signals output from the equipment satisfy the Poisson distribution in counting rate and the probability density function distribution of the reference spectrum in amplitude through the random sampling, which abides by the distribution law of the step ramp signals output by semiconductor X-ray detector. The spectrum generator is connected to a PC to change the reference spectral data and the signal output speed in real time. The control software of the PC is designed based on C++ programming. In addition, the reference spectral data of Ag, Fe, Cu and Zn characteristic X-rays are stored within the FPGA, so that a spectrum generator offline can still output the step ramp signals which satisfy the distributionpreviously mentioned in amplitude

The X-ray spectrum generator designed can be used to measure the system response function of X-ray fluorometer under different counting rates. Combined with the system response function and the inverse convolution method, it can eliminate the adverse impact of the ballistic deficit and electronics noise of X-ray fluorometer on the energy resolution, with improved energy resolution of the system. This X-ray spectrum generator can also be used to measure the maximum pulse passing rate, energy linearity, spectral line energy range and dead time of X-ray fluorometer.

[1] Wang N X and Zheng H W. Nucl Sci Tech, 2006, **17**: 11–15.
[2] Ge L Q, Zhou S C, Lai W C. In–Situ X Radiation Sampling Technique. Chengdu (China): Sichuan Science and Technology Press, 1997, 33–66, 150–212. (in Chinese)
[3] Fernández Timón A, Jurado Vargas M, Martín Sánchez A. Appl Radiat Isotop, 2010, **68**: 941–945.
[4] Wang J J, Fan T M, Qian Y G. Nuclear Electronics. Beijing (China): Atomic Energy Press, 1983, 158–170. (in Chinese)
[5] Gal J, Hegyesi G, Kalink G, *et al*. Nucl Instrum Meth A, 1997, **399**: 407–413.
[6] Zhou C Y, Su H, Kong J, *et al*. Nucl Sci Tech, 2012, **23**: 239–241.
[7] He Z S. Signals and systems. Higher Education Press, 2008, 48–86. (in Chinese)
[8] Cheng X, Han C, Mats P, *et al*. Nucl Instrum Meth A, 2013, **715**: 11–17.
[9] Fudan University, *et al*. Experimental Nuclear Physics. Beijing (China): Atomic Energy Press, 1985, 1–26. (in Chinese)
[10] Attwenger W, Gruber G, Patzelt R. Nucl Instrum Methods, 1969, **70**: 103–105.
[11] Byung yangAhn. in Proc.IEEE Asia Pacific Conference on Circuits and Systems, 1996, **11**:18– 21.
[12] Pan D J. Atom Energy Sci Technol, 1986, **4**: 431–434.(in Chinese)
[13] International Electrotechnical Commission, IEC: standard No. 659, Edition, 1980.
[14] Ziegler F, Beck D, Brand H. Nucl Instrum Meth A, 2012, **679**: 1–6.
[15] Wiernik M. Nucl Instrum Methods, 1971, **96**: 325–329.
[16] Mattingly J K and Mihalczo J T. Tennessee: Nuclear Materials Management and Storage Program Office March 13, 1998,1.
[17] Hamers H C and Marseille A. Physica, 1956, **22**: 563–568.
[18] Analog Devices. 16-Bit 30MSPS D/A Converter AD768 Data Sheet.
[19] Texas Instruments. Wideband, Current Feedback Operational Amplifier with Disable OPA 691 Data sheet.
[20] Du X F and Wu J. J Univer Sci and Technol China, 2006, **9**: 990–994. (in Chinese)